

## FTO demethylates YAP mRNA promoting oral squamous cell carcinoma tumorigenesis

Dian-Qi LI, Ci-Cheng HUANG, Guang ZHANG, Lei-Lei ZHOU\*

Department of Oral and Maxillofacial Surgery, Tongji Hospital of Tongji Medical College, Huazhong University of Science and Technology, Wuhan, China

\*Correspondence: llz\_tjh@yeah.net

Received July 16, 2021 / Accepted October 15, 2021

N<sup>6</sup>-methyladenosine (m<sup>6</sup>A) is the most common internal reversible modification of mRNA, which occurs on the N<sup>6</sup> nitrogen of adenosine. Fat mass and obesity-associated (FTO) is a demethylase that erases m<sup>6</sup>A modification and has recently been linked to cancer. Herein, we explored the role of FTO in oral squamous cell carcinoma (OSCC). High FTO mRNA and protein levels were observed in OSCC cell lines and tissues as compared to normal controls. OSCC patients with high FTO displayed larger tumor size, higher TNM stage, poorer differentiation, and shorter survival time than those with low FTO. Stable knockdown of FTO inhibited OSCC cell viability, colony formation, and tumor growth. Further, FTO depletion increased YAP1 m<sup>6</sup>A modification at mRNA 3'-untranslated region, accelerating the degradation of YAP1 mRNA, a well-documented oncogene promoting OSCC progression. Importantly, nucleocytoplasmic shuttling of FTO is critical for YAP1 mRNA demethylation and decay following YTHDF2 reading and recognition. Our results highlight the role of FTO in regulating YAP1 mRNA stability, and targeting of FTO/YAP1 axis may be a promising intervention for OSCC patients.

*Key words:* FTO, YAP1, OSCC, m<sup>6</sup>A modification, prognosis

Oral squamous cell carcinomas (OSCC) are a heterogeneous group of cancers arising from the mucosal lining of the oral cavity [1], with a high incidence worldwide in South Central Asia [2]. The primary modality of treatment for OSCC is surgery, chemotherapy, radiotherapy, or a combination of these modalities, depending on the extent of the disease and the patient's co-morbidity [3]. Although good progress has been made in the diagnosis and treatment of OSCC in recent years, the overall survival of OSCC is still not optimistic [4]. Hence, it is imminent to explore the biological mechanism of OSCC tumorigenesis for providing novel potential therapeutic targets.

N<sup>6</sup>-methyladenosine (m<sup>6</sup>A) modification is one of the most common epigenetic modifications of RNA molecules [5]. This process is reversible, aberrant m<sup>6</sup>A modification leads to the occurrence, development, and invasion of a variety of human cancers, and related regulators or inhibitors may bring potential strategies for the treatment of malignant tumors [6]. Up to date, some enzymes were shown to be involved in the dynamic process of m<sup>6</sup>A modification, including m<sup>6</sup>A methyltransferase, demethylase and binding protein, which are responsible for catalytic generation and elimination of m<sup>6</sup>A methylation and the specific recognition

of m<sup>6</sup>A site, respectively [7]. The consensus RRACH motif (R=G or A; H=A, C, or U) on endogenous RNA is required for m<sup>6</sup>A methylation, once methylated, RNA splicing, transport, expression, and translation may be affected, enabling m<sup>6</sup>A modification as a key player in the regulation of cell metabolism and various life processes [8].

Fat mass and obesity associated (FTO) (Uniprot: Q9C0B1), as the first discovered m<sup>6</sup>A demethylase, belongs to the alpha-ketoglutarate-dependent dioxygenase (ALKB) protein family and is associated with obesity [9]. In 1999, the FTO gene was first cloned in mice, and studies have confirmed that when the FTO gene is mutated, it increases the risk of obesity [10]. Knockout or overexpression of FTO significantly changes the bodyweight of mice [11]. Increasing evidence reveals a link between FTO and the occurrence, development, and prognosis of various cancers, no longer limited to obesity, diabetes, and other generational diseases [12]. However, its role in OSCC remains mysterious. In this study, we characterized the biological effect of FTO in OSCC. We found that FTO was significantly elevated in OSCC cell lines and tissues, it promoted OSCC progression by regulating yes-associated protein 1 (YAP1) (Uniprot: P46937) mRNA stability. YAP1, the main effector molecule downstream of the Hippo

signaling pathway, is frequently hyperactivated in human cancer, which promotes tumorigenesis via entering the nucleus to transcriptionally activate some proto-oncogenes (such as CTGF and CYR61) [13]. Therefore, our study provides new insights into the pathogenesis of OSCC.

## Materials and methods

**OSCC cell lines and tissues.** Five OSCC cell lines including SCC9, SCC25, CAL27, HN4, TSCCA and one human oral keratinocytes (HOK) cells were adherent cells and purchased from ATCC (Manassas, VA, USA), and cultured in Dulbecco's Modified Eagle Medium (DMEM) with high glucose, 10% fetal bovine serum (FBS), 100 U/ml penicillin and 0.1mg/ml streptomycin. They were frozen in liquid nitrogen for long-term storage after conventional passage. A total of 70 paired OSCC and paracancerous normal tissues (>2 cm from the edge of OSCC tissues) were retrospectively collected in this study for detecting FTO and YAP levels. Their lesions were surgically removed from 2014 to 2020 at Tongji Hospital of Tongji Medical College. All tissues were pathologically confirmed as OSCC. After they were discharged, the follow-up was performed by telephone or SMS (the survival time: 0.4–73.2 months). We obtained informed consent from all the patients, and this study was approved by the institutional review board and ethics committee of Tongji Hospital of Tongji Medical College (No. HWU00859-2).

**RT-qPCR assay.** Total RNA extraction was conducted by using TRIzol reagent (Invitrogen, Carlsbad, CA, USA) following the manufacturer's instructions. The concentration and quality of RNA were determined by NanoDrop 2000 (Thermo Fisher Scientific, Waltham, MA, USA), followed by DNA digestion using DNase I. The cDNA was reverse transcribed with 1 µg total RNA, amplification and quantifi-

cation were performed by using One Step TB Green<sup>®</sup> Prime-Script<sup>™</sup> RT-PCR Kit (Perfect Real Time) (Takara, Otsu, Japan) with specific primers on Applied Biosystems 7300 Real-Time PCR System (Thermo Fisher Scientific). Tubulin mRNA was used as the reference control, and the results were shown as relative values. The experiment was repeated three times with three replicates.  $2^{-\Delta\Delta Ct}$  formula was used to calculate gene relative level. The primer sequences are as follows: FTO mRNA: 5'-CAGCTTCTGGAAGCAAAACC-3' (Forward), 5'-GACCCGGGTGCTACAATCTA-3' (Reverse); YAP1 mRNA: 5'-CACAGCATGTTTCGAGCTCAT-3' (Forward), 5'-GATGCTGAGCTGTGGGTGTA-3' (Reverse); Tubulin mRNA: 5'-GACCAAGCGTACCATCCAGT-3' (Forward), 5'-CACGTTTGGCATAATCAGG-3' (Reverse).

**Western blot and immunohistochemistry (IHC).** Total protein was extracted by RIPA buffer. After quantification using Rapid Gold BCA Protein Quantification Kit (Thermo Fisher Scientific), 10 µg of proteins were loaded onto an SDS-PAGE gel. When the colored marker protein was separated to the appropriate position, the protein signal was transferred onto the PVDF membrane, followed by blocking using 5% non-fat milk powder. The membrane was incubated with anti-FTO (#ab126605, Abcam, Cambridge, UK; 1/10000 dilution), anti-YAP1 (#ab56701, Abcam; 1/1000 dilution) and anti-alpha Tubulin (#ab7291, Abcam; 1/5000 dilution) overnight at 4°C. After incubating with goat IgG H&L secondary antibody at 37°C for 1 h, the blot was developed using SuperSignal ECL detection reagents (Thermo Fisher Scientific). For IHC staining, the paraffin-embedded sections were made by the pathology department of Tongji Hospital of Tongji Medical College, after dewaxing, dehydration and, antigen retrieval using sodium citrate buffer (pH 6.0), IHC staining was performed with the Super Plus Hypersensitivity Rapid Immunohistochemical Assay Kit (Elabscience, Shanghai, China) following the supplier's instruction. The results were assessed by two experienced pathologists using the H-score method [14].

**Stable knockdown of FTO.** Lentivirus-mediated short hairpin RNA targeting FTO was inserted into the psi-LVRU6GP (GeneCopoeia, Rockville, MD, USA) vector, followed by transfection into SCC25 and CAL27 cells. After 72 h, the green fluorescence signal was observed under a fluorescence microscope. The stable cell lines were screened by using puromycin and were verified by qRT-PCR and western blot assays.

**CCK-8 and colony formation assays.** For the CCK-8 assay, OSCC cells were plated onto 96-well plates and then cultured three days following treatment with 10 µl CCK-8 reagent (Dojindo, Kumamoto, Japan). The absorbance at 450 nm reflected cell viability. For colony formation assay, cells were seeded onto 6-well plates and cultured for 2 weeks. Then, cells were stained by crystal violet.

**Nude mice assay.** A total of 6 mice aged 4–6 weeks were purchased from Shanghai Experimental Animal Center, Chinese Academy of Sciences (Shanghai, China), and

**Table 1. The correlations between FTO protein expression and clinicopathological characteristics of patients with OSCC.**

Parameters	All cases (n=70)	FTO expression		p-value
		Low (n=35)	High (n=35)	
Age (years)				
≤60	32	18	14	0.337
>60	38	17	21	
Gender				
Male	35	15	20	0.232
Female	35	20	15	
Tumor size				
≤3 cm	41	26	15	0.008
>3 cm	29	9	20	
TNM stage				
I–II	47	28	19	0.022
III–IV	23	7	16	
Tumor differentiation				
Well/Moderate	28	23	5	<0.001
Poor	42	12	30	

randomly divided into 2 groups (n=3/group). FTO-silenced SCC25 cells were injected subcutaneously into mice. After 5 weeks, all mice were sacrificed and tumor tissues were weighed and photographed.

**Luciferase reporter assay.** *YAP1* 3'-UTR containing four predicted m<sup>6</sup>A motifs were synthesized and inserted into the pmirGLO vector (Promega, Madison, WI, USA), followed by transfection into control and FTO-silenced cells using Lipofectamine 2000 (Invitrogen). The mutation from adenine to guanine was conducted by TaKaRa MutanBEST Kit (TaKaRa) as per the supplier's instructions. The luciferase activity was detected using the Dual-Luciferase Reporter Assay System (Promega).

**Methylated RNA immunoprecipitation (MeRIP) assay.** MeRIP assay was conducted by using the Magna MeRIP m<sup>6</sup>A Kit (Millipore, Schwalbach, Germany) following the supplier's instructions. In brief, total RNA was extracted using miRNeasy Mini Kit (Qiagen, Dusseldorf, Germany) with stringent DNA digestion, followed by chemical fragmentation to about 100 nt. RNA was then immunoprecipitated with 5 µg m<sup>6</sup>A antibody or anti-mouse IgG linked to protein A/G magnetic beads. After elution, m<sup>6</sup>A enrichment on *YAP1* mRNA 3'-UTR was analyzed by qRT-PCR normalizing to input (10% fragmented RNA).

**Immunofluorescence.** The wild-type and mutant FTO cDNA full-length sequences were amplified by PCR and fused into pCMV3-N-His Vector (Sino Biological, Wayne,

PA, USA) via seamless cloning. Then, OSCC cells were transfected with the above vectors using Lipofectamine 2000. Cells were washed with PBS and fixed with 4% paraformaldehyde for 30 min at room temperature. After blocking with 5% BSA, cells were incubated with anti-His tag (#ab9108, Abcam, 1/100 dilution) at 4°C overnight. Next, cells were incubated with goat anti-rabbit IgG H&L (Alexa Fluor® 488) (#ab150077, Abcam; 1/500 dilution) at room temperature in the dark for 1 h. 4',6-diamidino-2-phenylindole (DAPI, Beyotime, Beijing, China) was used to stain the nuclei. The green fluorescence signal was observed under a fluorescence microscope.

**Statistical analysis.** All data were analyzed and figures were generated using GraphPad Prism 8 software and shown as mean ± standard deviation (SD) of at least three independent experiments carried out in triplicate. The correlation between FTO level and OSCC survival time was determined by the Kaplan-Meier plotter. A two-tailed Student's t-test was used to assess the difference between the two groups. A p-value <0.05 was considered statistically significant.

## Results

**FTO is significantly upregulated in OSCC cell lines and tissues.** As shown in Figure 1A, *FTO* mRNA was highly expressed in five OSCC cell lines as compared to

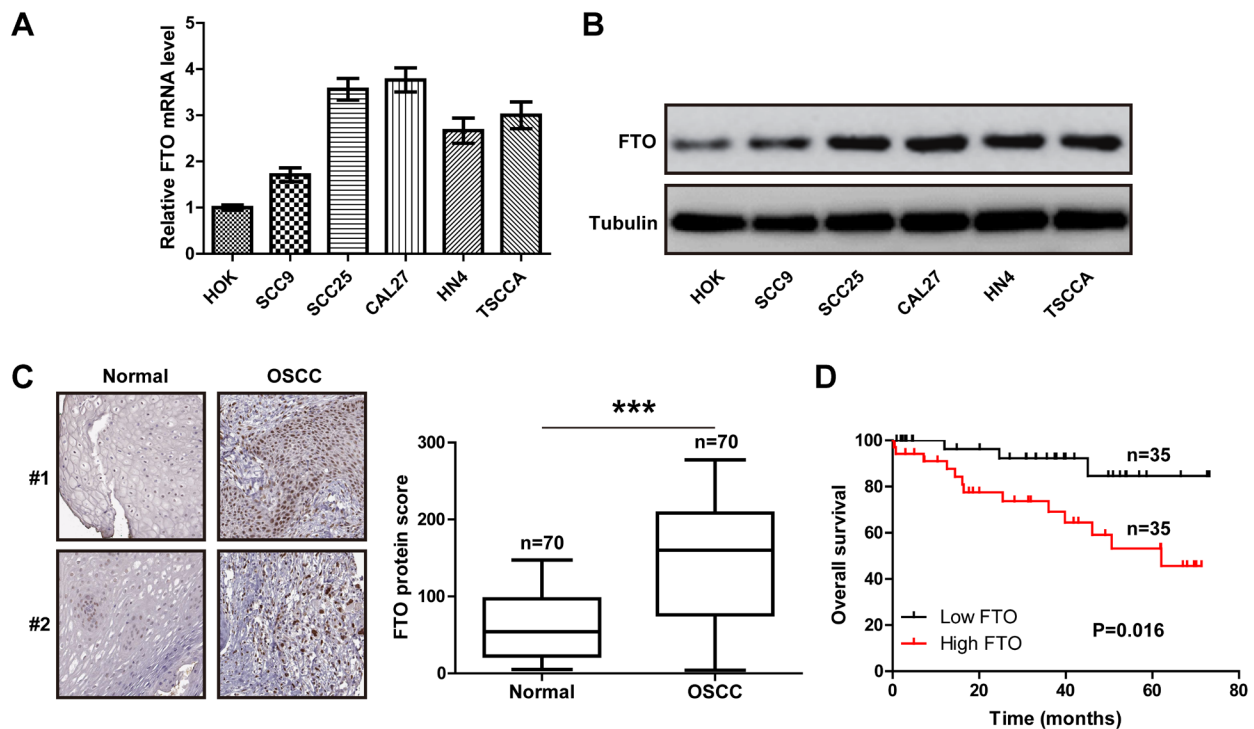


**Figure 1.** FTO is upregulated in OSCC cell lines and tissues. A, B) qRT-PCR and western blot assays testing FTO mRNA and protein levels in the indicated cell lines, respectively. C) IHC staining of FTO protein levels in 70 paired OSCC and normal tissues, a left panel showing the two cases of representative staining results. D) The survival curve of OSCC patients with low (n=35) and high (n=35) FTO levels (Log-rank test). \*\*\*p<0.001

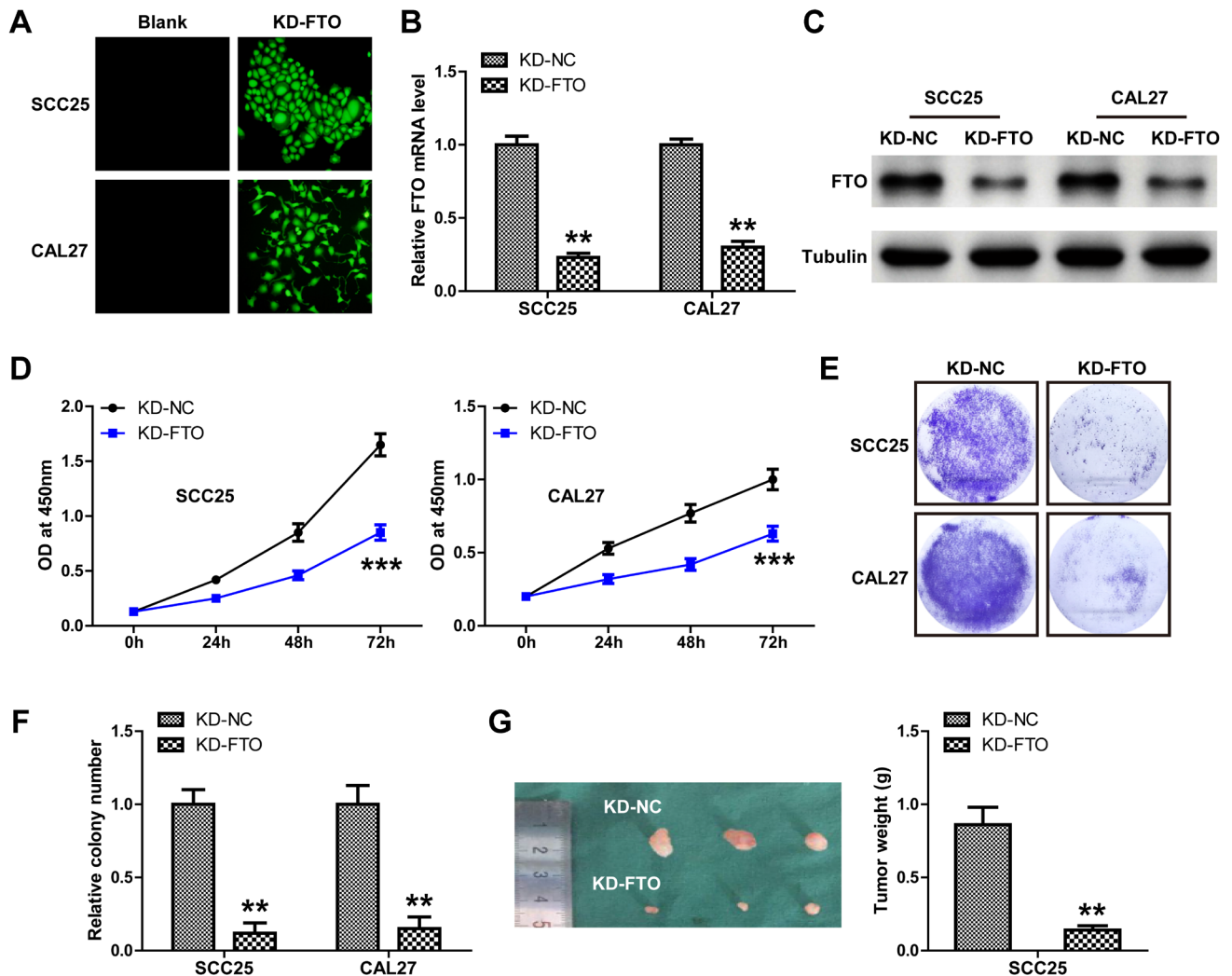


**Figure 2.** Stable knockdown of FTO inhibits OSCC cell growth. A) OSCC cell lines were infected by the shFTO lentiviral vector with GFP tag and observed under the fluorescence microscope. B, C) qRT-PCR and western blot assays verifying infection efficiency (n=3, a two-tailed Student's t-test). D-F) Cell proliferation was assessed by CCK-8 and colony formation assays (n=3, a two-tailed Student's t-test). G) The image and weight of the subcutaneous tumor in control and FTO-silenced groups (n=3, a two-tailed Student's t-test). Abbreviations: KD-Knock down; NC-negative control; \*\* $p < 0.01$ ; \*\*\* $p < 0.001$

normal HOK cells, with the highest expression in SCC25 and CAL27 cells. And FTO protein level displayed a similar trend (Figure 1B). Next, we collected a total of 70 paired OSCC and normal tissues, IHC staining showed that FTO positive cells (positive in the nuclei) in OSCC tissues were significantly more than those in normal tissues (Figure 1C). High FTO levels were positively correlated with larger tumor size ( $p=0.008$ ), advanced TNM stage ( $p=0.022$ ), and poor tumor differentiation ( $p < 0.001$ , Table 1). More importantly, patients with a high FTO expression showed a shorter overall survival time than patients with a low FTO expression ( $p=0.016$ , Figure 1D).

**Depletion of FTO inhibits OSCC cell proliferation both *in vitro* and *in vivo*.** To explore the effect of FTO

on OSCC cells, we generated two FTO stably knockdown cell lines with the highest FTO levels using a lentiviral vector (Figure 2A), which was verified by qRT-PCR and western blot assays (nearly four-fold reduction) (Figures 2B, 2C). CCK-8 showed that cell viability was significantly decreased after the FTO knockdown ( $p < 0.001$ , Figure 2D) at the indicated time. Moreover, the colony formation assay showed that fewer colonies were formed in FTO-depleted SCC25 and CAL27 cells in comparison to control cells ( $p < 0.01$ , Figures 2E, 2F). Furthermore, we established the xenograft tumor model using nude mice, the results showed that the weight of subcutaneous tumor in the FTO knock-down group was lighter than that in the control group ( $p < 0.01$ , Figure 2G).

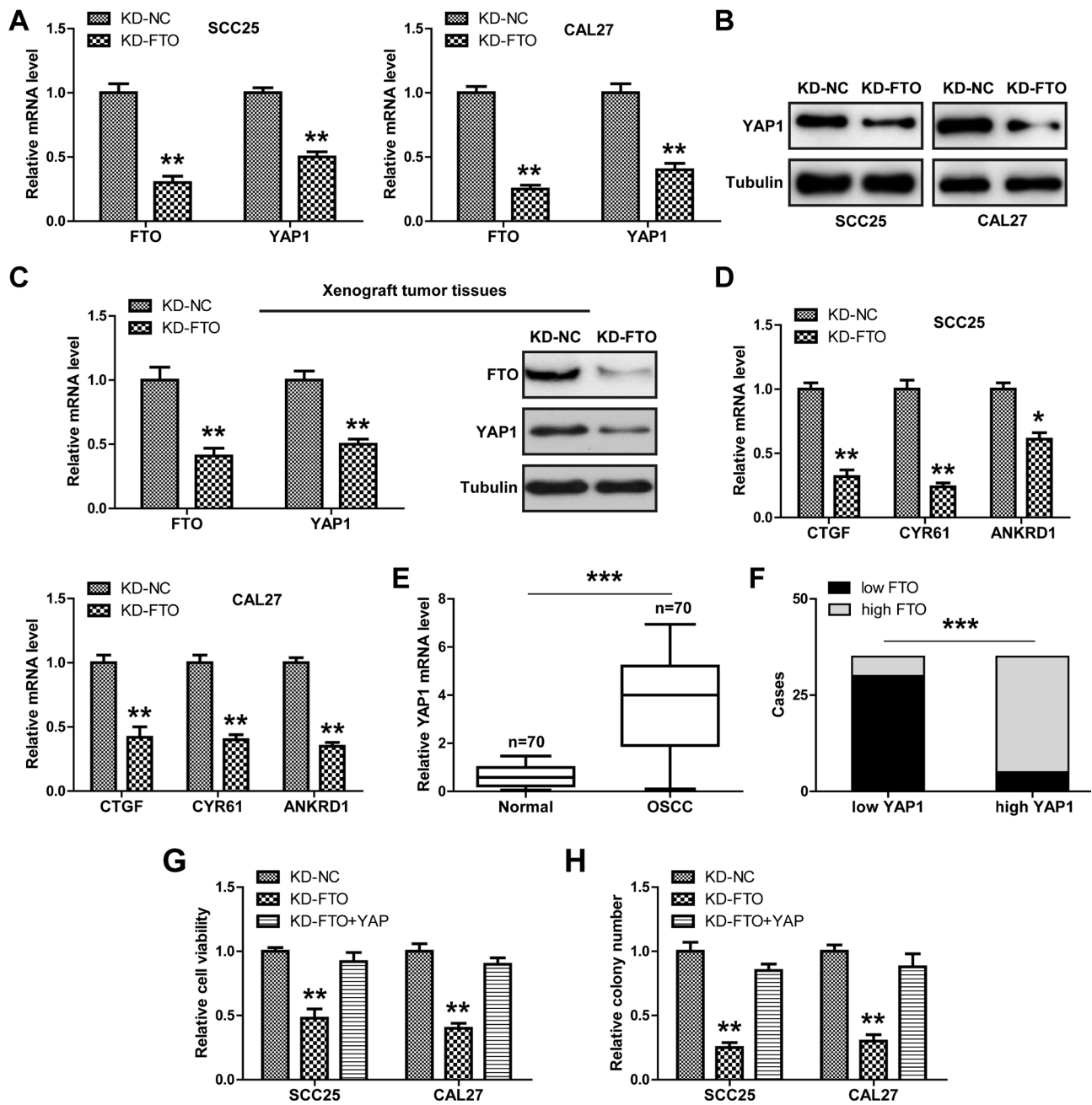


**Figure 3.** FTO upregulates YAP1 expression. A, B) Analysis of YAP1 mRNA and protein levels after FTO knockdown (n=3, a two-tailed Student's t-test). C) YAP1 mRNA and protein levels in xenograft tumor tissues with FTO knockdown (n=3, a two-tailed Student's t-test). D) qRT-PCR analysis of the indicated gene expression in FTO-silenced cell lines (n=3, a two-tailed Student's t-test). E) qRT-PCR analysis of YAP1 mRNA expression in 70 matched OSCC and normal tissues. F) The correlation between FTO and YAP1 expression in OSCC tissues (n=3, a two-tailed Student's t-test). G, H) Cell proliferation assay in FTO-silenced cell lines after YAP1 overexpression (n=3, a two-tailed Student's t-test). Abbreviations: KD-Knock down; NC-negative control; \*p<0.05, \*\*p<0.01; \*\*\*p<0.001

**YAP1 is the downstream target of FTO in OSCC cells.** Considering that YAP1 is an important oncogene in OSCC, we hypothesized that FTO might play a role through YAP1. As expected, knockdown of *FTO* dramatically reduced *YAP1* mRNA and protein levels in both SCC25 and CAL27

cells (p<0.01, Figures 3A, 3B), and these results were also confirmed in the xenograft tumor model (p<0.01, Figure 3C). Consistently, some well-known YAP1 targets including CTGF, CYR61, and ANKRD1 were nearly two-fold downregulated after FTO silencing (p<0.01, Figure 3D). Besides, high

*YAP1* was found in OSCC tissues ( $p < 0.001$ , Figure 3E) as compared to normal tissues, and its expression was closely positively correlated with *FTO* expression ( $p < 0.001$ , Figure 3F). Functionally, overexpression of *YAP1* in *FTO*-silenced OSCC cells could effectively rescue the weakened cell viability and colony ability caused by *FTO* knockdown ( $p < 0.01$ , Figures 3G, 3H).

**FTO stabilizes *YAP1* mRNA via erasing m<sup>6</sup>A modification.** Given that m<sup>6</sup>A-modified mRNA is easy to degrade, we then wondered whether *FTO* affected *YAP1* mRNA stability. SCC25 and CAL27 cells were treated with actinomycin D, an RNA synthesis inhibitor, followed by qRT-PCR analysis. The results showed that the half-life of *YAP1* mRNA in *FTO*-silenced cells was nearly 2 h shorter than that in control cells ( $p < 0.01$ , Figure 4A). Through analyzing the SRAMP online database (<http://www.cuilab.cn/sramp>), we found 4 m<sup>6</sup>A modification sites (AGACU, GAACA, AAACU, AGACU) with very high confidence located on *YAP1* mRNA 3'-UTR (Figure 4B). The sequence was then cloned into the

pmirGLO reporter to conduct a luciferase reporter assay (Figure 4C). As shown in Figures 4D and 4E, the luciferase activity was two-fold attenuated by knockdown of *FTO*, while mutation of m<sup>6</sup>A motifs abolished this effect ( $p < 0.01$ ). Consistently, *FTO* knockdown notably increased m<sup>6</sup>A levels on *YAP1* mRNA ( $p < 0.01$ , Figure 4F). Since YTHDF2 can recognize cytoplasmic m<sup>6</sup>A, leading to mRNA degradation, we then inferred that YTHDF2 was involved in *YAP1* mRNA turnover. qRT-PCR results showed that the reduced *YAP1* mRNA caused by *FTO* depletion was evidently blocked after the knockdown of YTHDF2 in these two OSCC cell lines ( $p < 0.01$ , Figure 4G).

**Subcellular localization of *FTO* is critical for *YAP1* mRNA demethylation.** Then, we transfected OSCC cells with His-tag *FTO* wild type (WT) and *FTO* T150E (Thr-to-Glu mutation imitating the phosphorylated form of *FTO*) vectors. Immunofluorescence showed that *FTO* WT mainly displayed a nuclear localization, while *FTO* T150E displayed a cytosolic localization (Figure 5A). MeRIP assay showed

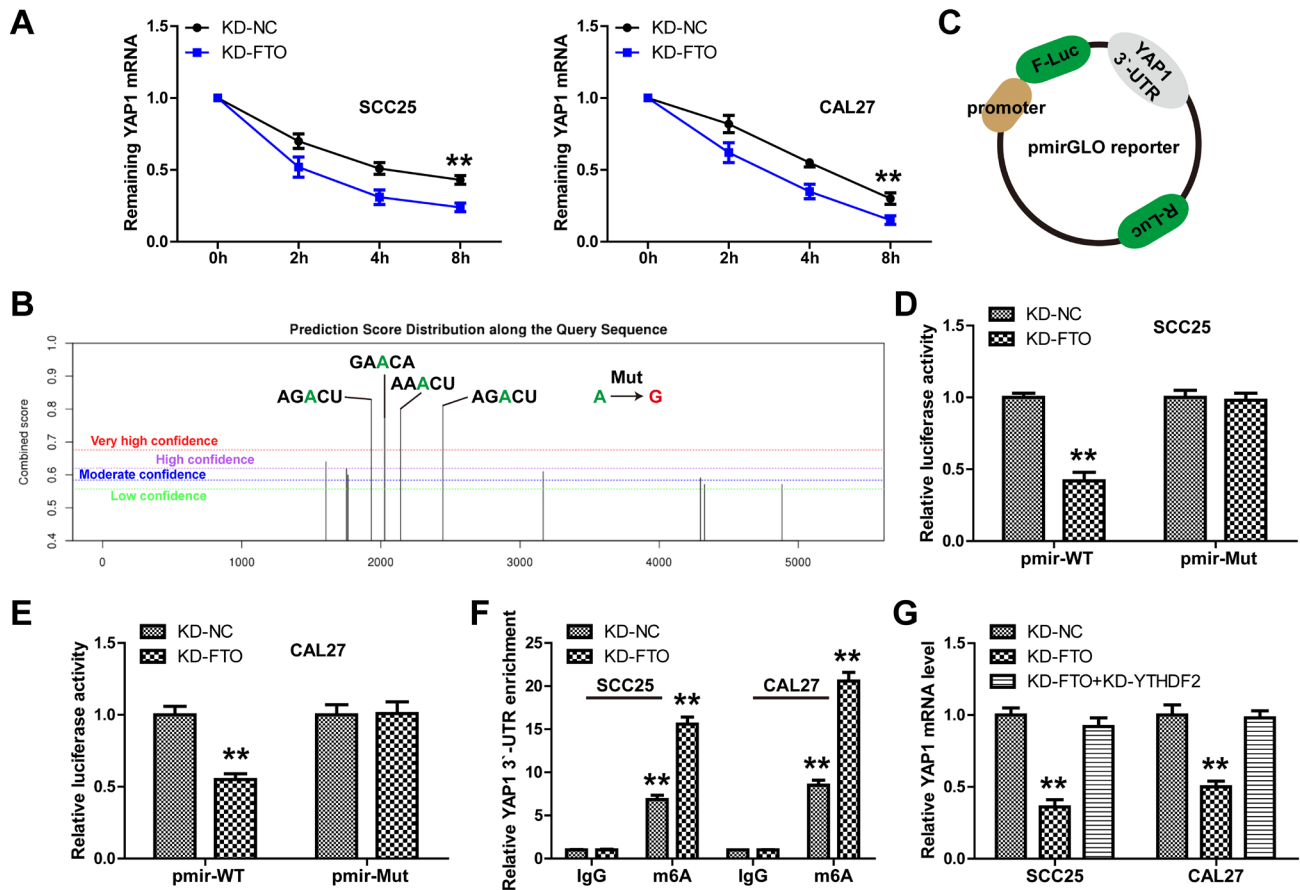


**Figure 4.** FTO demethylates *YAP1* mRNA. **A**) qRT-PCR analysis of the remaining *YAP1* mRNA after treatment with actinomycin D at the indicated time ( $n=3$ , a two-tailed Student's *t*-test). **B**) The SRAMP database predicting the m<sup>6</sup>A motifs on *YAP1* mRNA. **C–E**) *YAP1* 3'-UTR containing four m<sup>6</sup>A motifs were cloned into the pmirGLO vector, followed by a luciferase reporter assay ( $n=3$ , a two-tailed Student's *t*-test). **F**) The MeRIP assay testing m<sup>6</sup>A enrichment on *YAP1* 3'-UTR after *FTO* knockdown. **G**) qRT-PCR analysis of *YAP1* mRNA level in *FTO*-silenced cell lines transfection with YTHDF2 siRNA ( $n=3$ , a two-tailed Student's *t*-test). Abbreviations: KD-Knock down; NC-negative control; \*\* $p < 0.01$

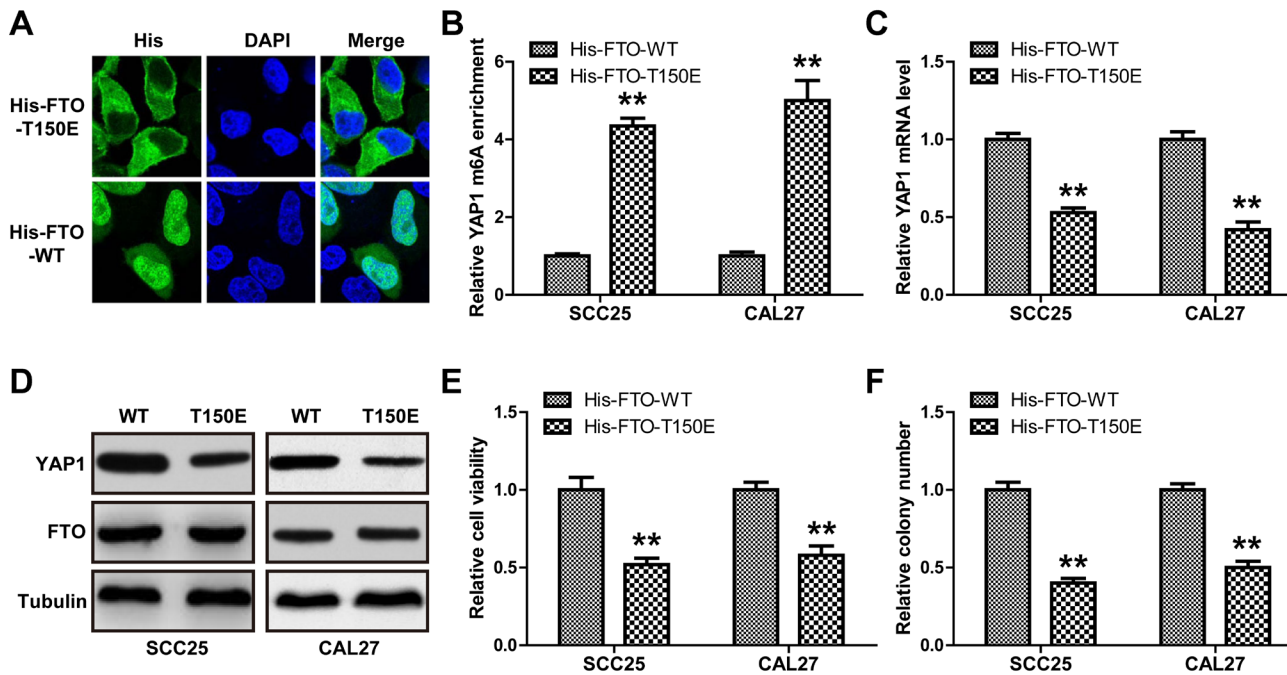


**Figure 5.** Nuclear localization of FTO is essential for YAP1 mRNA demethylation. **A)** Immunofluorescence testing the location of FTO after transfection with His-FTO-WT or His-FTO-T150E vector. **B, C)** MeRIP and qRT-PCR analysis detecting YAP1 3'-UTR m<sup>6</sup>A enrichment and YAP1 mRNA levels, respectively, in OSCC cells transfected with the indicated vectors (n=3, a two-tailed Student's t-test). **D)** Western blot assay testing YAP1 and FTO protein levels in cells transfected with the indicated vectors. **E, F)** Cell proliferation assay in cells transfected with the indicated vectors (n=3, a two-tailed Student's t-test). \*\*p<0.01

that FTO T150E increased about five-fold m<sup>6</sup>A enrichment on YAP1 mRNA 3'-UTR compared to FTO WT (p<0.01, Figure 5B), accompanied by downregulation of YAP1 mRNA and protein levels (p<0.01, Figures 5C, 5D), while total FTO protein level remained unchanged (Figure 5D). Functionally, the viability and colony formation ability of FTO T150E cells were significantly attenuated in comparison to FTO WT cells (p<0.01, Figures 5E, 5F).

## Discussion

In this study, we found that FTO was significantly increased in OSCC cell lines and tissues, and high FTO was closely correlated with poor prognosis. Knockdown of FTO remarkably inhibited OSCC cell growth both *in vitro* and *in vivo*. As a key m<sup>6</sup>A demethylase, FTO affects tumor cell growth, proliferation, differentiation, self-renewal, metastasis, radiotherapy, and chemotherapy sensitivity [15]. However, it functions differently or even in opposite ways in different contexts. For example, FTO was significantly increased in breast cancer [16], cervical cancer [17], lung cancer [18], and leukemia [19], contributing to cell malignant phenotype and aggressive progression. Nevertheless, some studies showed that FTO was lowly expressed in ovarian cancer [20] and gastric cancer [21], serving as a tumor suppressor. To the best of our knowledge, this is the first study character-

izing the oncogenic role of FTO in OSCC, which provides a theoretical basis for FTO as a potential clinical therapeutic target for OSCC patients.

Studies have shown that nucleoplasmic shuttle is essential for FTO function, FTO phosphorylation increases the cytoplasmic localization of FTO and loses its demethylation effect [22]. However, mRNA decay occurs in the cytoplasm, the cytoplasmic m<sup>6</sup>A "reader" may be responsible for its process. YTHDF2 belongs to the YT521-B homology (YTH) domain family and is a well-documented m<sup>6</sup>A "reader" that plays a fundamental role in multiple diseases, including cancer [23]. Unlike its two homologous analogs, YTHDF1 and YTHDF3, which affect mRNA translation, YTHDF2 is mainly able to recognize m<sup>6</sup>A mRNA in the cytoplasm and guide its degradation [24]. In YTHDF2 knockdown cells, the half-life of m<sup>6</sup>A-containing mRNA is increased by ~30% [25]. In this study, we found that YTHDF2 knockdown in OSCC cells could significantly block the reduced YAP1 mRNA levels caused by FTO silencing, implying that YTHDF2 recognizes cytoplasmic m<sup>6</sup>A YAP1 mRNA and increases YAP1 degradation. Further studies are needed to expound on the physiological role of FTO phosphorylation in OSCC and which specific factors or signal pathways control its phosphorylation and nucleocytoplasmic distribution.

Hippo signaling pathway is composed of a group of conserved kinases that inhibits cell growth [26]. In mammals,

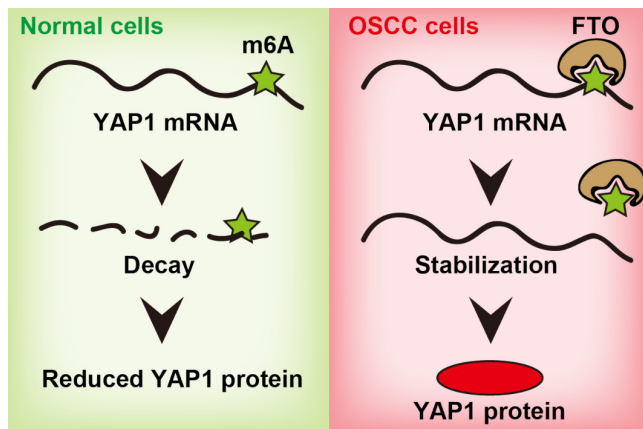


Figure 6. The model showing the oncogenic role of FTO in OSCC via regulation of YAP1 mRNA m<sup>6</sup>A level.

activation of the Hippo signaling acts on downstream effect factors YAP1 and TAZ through a series of phosphorylation reactions of kinases, resulting in YAP1 cytoplasmic retention, which cannot enter the nucleus to exert its transcriptional activation function [27]. Emerging evidence suggests that YAP1 is frequently overexpressed in various human cancers, including OSCC [28]. YAP1 is able to activate a cohort of oncogenes, such as CTGF and CYR61, leading to cancer progression [29]. Studies on the regulation of YAP1 mainly focus on post-translational modification, phosphorylation, ubiquitination, etc. [30], and little is known about its post-transcriptional regulation. Herein, through using bioanalysis, we found four high confidence m<sup>6</sup>A motifs on YAP1 mRNA 3'-UTR. The MeRIP assays showed that FTO bound directly to these sites, and mutation of these motifs increased the luciferase reporter activity, suggesting that FTO increases YAP1 mRNA stability via these motifs. Hence, our data provide a novel epigenetic mechanism governing YAP1 expression at the post-transcriptional level (Figure 6). Whether this FTO/YAP1 axis also exists in other malignant tumors remains to be further explored.

In summary, our findings for the first time reveal the carcinogenic effect of m<sup>6</sup>A demethylase FTO in OSCC and provide a potential prognostic biomarker, which needs to be verified by other multi-center large samples surveys. The dysregulation of the previously uncharacterized axis of FTO/YAP1 may be critical for OSCC development and progression.

## References

- NEVILLE BW, DAY TA. Oral cancer and precancerous lesions. *CA Cancer J Clin* 2002; 524: 195–215. <https://doi.org/10.3322/canjclin.52.4.195>
- SUNG H, FERLAY J, SIEGEL RL, LAVERSANNE M, SOERJOMATARAM I et al. Global Cancer Statistics 2020: GLOBOCAN Estimates of Incidence and Mortality Worldwide for 36 Cancers in 185 Countries. *CA Cancer J Clin* 2021; 713: 209–249. <https://doi.org/10.3322/caac.21660>
- STEIGEN SE, SOLAND TM, NGINAMAU ES, LAURVIK H, COSTEA DE et al. Grading of oral squamous cell carcinomas – Intra and interrater agreeability: Simpler is better? *J Oral Pathol Med* 2020; 497: 630–635. <https://doi.org/10.1111/jop.12990>
- LUBPAIREE T, POH CF, LARONDE DM, ROSIN MP, ZHANG L. Oral Squamous Cell Carcinomas are Associated with Poorer Outcome with Increasing Ages. *J Oncol Res Ther* 2017; 34.
- FU Y, DOMINISSINI D, RECHAVI G, HE C. Gene expression regulation mediated through reversible m(6)A RNA methylation. *Nat Rev Genet* 2014; 155: 293–306. <https://doi.org/10.1038/nrg3724>
- SUN T, WU R, MING L. The role of m6A RNA methylation in cancer. *Biomed Pharmacother* 2019; 112: 108613. <https://doi.org/10.1016/j.biopha.2019.108613>
- GUI Y, YUAN S. Epigenetic regulations in mammalian spermatogenesis: RNA-m(6)A modification and beyond. *Cell Mol Life Sci* 2021; 78: 4893–4905. <https://doi.org/10.1007/s00018-021-03823-9>.
- UDDIN MB, WANG Z, YANG C. The m(6)A RNA methylation regulates oncogenic signaling pathways driving cell malignant transformation and carcinogenesis. *Mol Cancer* 2021; 201: 61. <https://doi.org/10.1186/s12943-021-01356-0>
- FRAYLING TM, TIMPSON NJ, WEEDON MN, ZEGGINI E, FREATHY RM et al. A common variant in the FTO gene is associated with body mass index and predisposes to childhood and adult obesity. *Science* 2007; 3165826: 889–894. <https://doi.org/10.1126/science.1141634>
- CHURCH C, LEE S, BAGG EA, MCTAGGART JS, DEACON R et al. A mouse model for the metabolic effects of the human fat mass and obesity associated FTO gene. *Plos Genet* 2009; 58: e1000599. <https://doi.org/10.1371/journal.pgen.1000599>
- MCMURRAY E, CHURCH CD, LARDER R, NICHOLSON G, WELLS S et al. Adult onset global loss of the fto gene alters body composition and metabolism in the mouse. *Plos Genet* 2013; 91: e1003166. <https://doi.org/10.1371/journal.pgen.1003166>
- CHEN J, DU B. Novel positioning from obesity to cancer: FTO, an m(6)A RNA demethylase, regulates tumour progression. *J Cancer Res Clin Oncol* 2019; 1451: 19–29. <https://doi.org/10.1007/s00432-018-2796-0>
- NGUYEN C, YI C. YAP/TAZ Signaling and Resistance to Cancer Therapy. *Trends Cancer* 2019; 55: 283–296. <https://doi.org/10.1016/j.trecan.2019.02.010>
- DETRE S, SACLANI JG, DOWSETT M. A “quickscore” method for immunohistochemical semiquantitation: validation for oestrogen receptor in breast carcinomas. *J Clin Pathol* 1995; 489: 876–878. <https://doi.org/10.1136/jcp.48.9.876>
- WANG JY, CHEN LJ, QIANG P. The Potential Role of N6-Methyladenosine (m6A) Demethylase Fat Mass and Obesity-Associated Gene (FTO) in Human Cancers. *Onco Targets Ther* 2020; 13: 12845–12856. <https://doi.org/10.2147/OTT.S283417>
- NIU Y, LIN Z, WAN A, CHEN H, LIANG H et al. RNA N6-methyladenosine demethylase FTO promotes breast tumor progression through inhibiting BNIP3. *Mol Cancer* 2019; 181: 46. <https://doi.org/10.1186/s12943-019-1004-4>

- [17] ZOU D, DONG L, LI C, YIN Z, RAO S et al. The m(6)A eraser FTO facilitates proliferation and migration of human cervical cancer cells. *Cancer Cell Int* 2019; 19: 321. <https://doi.org/10.1186/s12935-019-1045-1>
- [18] LI J, HAN Y, ZHANG H, QIAN Z, JIA W et al. The m6A demethylase FTO promotes the growth of lung cancer cells by regulating the m6A level of USP7 mRNA. *Biochem Biophys Res Commun* 2019; 5123: 479–485. <https://doi.org/10.1016/j.bbrc.2019.03.093>
- [19] SU R, DONG L, LI C, NACHTERGAELE S, WUNDERLICH M et al. R-2HG Exhibits Anti-tumor Activity by Targeting FTO/m(6)A/MYC/CEBPA Signaling. *Cell* 2018; 172: 90–105.e23. <https://doi.org/10.1016/j.cell.2017.11.031>
- [20] HUANG H, WANG Y, KANDPAL M, ZHAO G, CARDENAS H et al. FTO-Dependent N(6)-Methyladenosine Modifications Inhibit Ovarian Cancer Stem Cell Self-Renewal by Blocking cAMP Signaling. *Cancer Res* 2020; 8016: 3200–3214. <https://doi.org/10.1158/0008-5472.CAN-19-4044>
- [21] LI Y, ZHENG D, WANG F, XU Y, YU H et al. Expression of Demethylase Genes, FTO and ALKBH1, Is Associated with Prognosis of Gastric Cancer. *Dig Dis Sci* 2019; 646: 1503–1513. <https://doi.org/10.1007/s10620-018-5452-2>
- [22] HIRAYAMA M, WEI FY, CHUJO T, OKI S, YAKITA M et al. FTO Demethylates Cyclin D1 mRNA and Controls Cell-Cycle Progression. *Cell Rep* 2020; 311: 107464. <https://doi.org/10.1016/j.celrep.2020.03.028>
- [23] WANG JY, LU AQ. The biological function of m6A reader YTHDF2 and its role in human disease. *Cancer Cell Int* 2021; 211: 109. <https://doi.org/10.1186/s12935-021-01807-0>
- [24] LEE Y, CHOE J, PARK OH, KIM YK. Molecular Mechanisms Driving mRNA Degradation by m(6)A Modification. *Trends Genet* 2020; 363: 177–188. <https://doi.org/10.1016/j.tig.2019.12.007>
- [25] WANG X, LU Z, GOMEZ A, HON GC, YUE Y et al. N6-methyladenosine-dependent regulation of messenger RNA stability. *Nature* 2014; 5057481: 117–120. <https://doi.org/10.1038/nature12730>
- [26] PAN D. The hippo signaling pathway in development and cancer. *Dev Cell* 2010; 194: 491–505. <https://doi.org/10.1016/j.devcel.2010.09.011>
- [27] MO JS, PARK HW, GUAN KL. The Hippo signaling pathway in stem cell biology and cancer. *Embo Rep* 2014; 156: 642–656. <https://doi.org/10.15252/embr.201438638>
- [28] MAEHAMA T, NISHIO M, OTANI J, MAK TW, SUZUKI A. The role of Hippo-YAP signaling in squamous cell carcinomas. *Cancer Sci* 2021; 1121: 51–60. <https://doi.org/10.1111/cas.14725>
- [29] SHIBATA M, HAM K, HOQUE MO. A time for YAP1: Tumorigenesis, immunosuppression and targeted therapy. *Int J Cancer* 2018; 1439: 2133–2144. <https://doi.org/10.1002/ijc.31561>
- [30] YAN F, QIAN M, HE Q, ZHU H, YANG B. The posttranslational modifications of Hippo-YAP pathway in cancer. *Biochim Biophys Acta Gen Subj* 2020; 18641: 129397. <https://doi.org/10.1016/j.bbagen.2019.07.006>